References

[1] G.W. Stachowiak, A.W. Batchelor, ENGINEERING TRIBOLOGY, Butterworth-Heinemann, USA, 2013.

[2] B. Bhushan, Introduction to Tribology, Second, John Wiley & Sons, New York, 2013.

[3] I. Hutchings, P. Shipway, Tribology: Friction and wear of engineering materials, Second, Butterworth-Heinemann,UK, Cambridge, 2017.

[4] T. Mang, K. Bobzin, T. Bartels, Industrial tribology: Tribosystems, friction, wear and surface engineering, lubrication, John Wiley & Sons, New York, 2011.

[5] S.S. Rawat, A.P. Harsha, Current and Future Trends in Grease Lubrication, in: S. Springer (Ed.), Automot. Tribol., Jaypee Brothers Medical Publishers (P) Ltd., Singapore, 2019: pp. 147–182. https://doi.org/10.1007/978-981-15-0434-1_9.

[6] A. Erdemir, Review of engineered tribological interfaces for improved boundary lubrication, Tribol. Int. 38 (2005) 249–256. https://doi.org/10.1016/j.triboint.2004.08.008.

[7] C. Pownraj, A. Valan Arasu, Effect of dispersing single and hybrid nanoparticles on tribological, thermo-physical, and stability characteristics of lubricants: a review, Springer International Publishing, 2021. https://doi.org/10.1007/s10973-020-09837-y.

[8] A.M. Rao, S.P. Srivastava, K.C. Mehta, Synthetic lubricants in India — an overview, J. Synth. Lubr. 4 (1987) 137–145. https://doi.org/10.1002/jsl.3000040204.

[9] T. Mang, Encyclopedia of Lubricants and Lubrication, Springer, New York, 2014. https://doi.org/10.1007/978-3-642-22647-2.

[10] M.M. Wu, S.C. Ho, T.R. Forbus, Synthetic lubricant base stock processes and products, in: Pract. Adv. Pet. Process., Springer, New York, 2006: pp. 553–577. https://doi.org/10.1007/978-0-387-25789-1.

[11] A.E. and K. Holmberg, Coating Technology for Vehicle Applications, Springer International Publishing, Cham, 2015. https://doi.org/10.1007/978-3-319-14771-0.

[12] M. Technology, Introduction to synthetic lubricants & their applications, Maint. Technol. (2007) 1–5. http://www.maintenancetechnology.com/2007/05/introduction-to-synthetic-lubricants-a-their-applications/.

[13] R.A.E. Wright, K. Wang, J. Qu, B. Zhao, Oil-Soluble Polymer Brush Grafted Nanoparticles as Effective Lubricant Additives for Friction and Wear Reduction, Angew. Chemie. 128 (2016) 8798–8802. https://doi.org/10.1002/ange.201603663.

[14] Z. Tang, S. Li, A review of recent developments of friction modifiers for liquid lubricants (2007-present), Curr. Opin. Solid State Mater. Sci. 18 (2014) 119–139. https://doi.org/10.1016/j.cossms.2014.02.002.

[15] X. Wu, K. Gong, G. Zhao, W. Lou, X. Wang, W. Liu, Surface Modification of MoS 2 Nanosheets as Effective Lubricant Additives for Reducing Friction and Wear in Poly-α-olefin, Ind. Eng. Chem. Res. 57 (2018) 8105–8114. https://doi.org/10.1021/acs.iecr.8b00454.

[16] W. Dai, B. Kheireddin, H. Gao, H. Liang, Roles of nanoparticles in oil lubrication, Tribol. Int. 102 (2016) 88–98. https://doi.org/10.1016/j.triboint.2016.05.020.

[17] I. Madanhire, C. Mbohwa, Mitigating Environmental Impact of Petroleum Lubricants, Springer International Publishing, Cham, 2016. https://doi.org/10.1007/978-3-319-31358-0.

[18] J. Trout, J. Fitch, Synthetic Oil: What Consumers Need to Know, Mach. Lubr. March (2020) 1–10. https://www.machinerylubrication.com/Articles/Print/31800.

[19] MarketsandMarketsTM, Synthetic Lubricants Market by Type (PAO, PAG, Esters, Group III), Application (Engine Oil, Hydraulic Fluids, Metalworking Fluids, Compressor Oil, Gear Oil, Refrigeration Oil, Transmission Fluids, Turbine Oil), Region - Global Forecast to 2023, MarketsandMarketsTM. (2019). https://www.marketsandmarkets.com/Market-Reports/synthetic-lubricant-market-141429702.html.

[20] M.C. Goze, A.I. Kramer, P.J. and Nandapurkar, N. Yang, Method of making low viscosity PAO, US 7.652,186, 2010.

[21] T. Mang, Encyclopedia of Lubricants and Lubrication, Springer Berlin Heidelberg,

Berlin, Heidelberg, 2014. https://doi.org/10.1007/978-3-642-22647-2.

[22] L.D. Moore, D.R. Fels, A.B. Seay, C. Lopez, K.E. Harris, D.A. Peck, PAO-based synthetic lubricants in industrial applications, Lubr. Eng. 59 (2003) 23–30.

[23] R.L. Shubkin, M.E. Kerkemeyer, Tailor-making polyalphaolefins, J. Synth. Lubr. 8 (1991) 115–134. https://doi.org/10.1002/jsl.3000080204.

[24] L.R. Rudnick, Synthetics, Mineral Oils, and Bio-Based Lubricants, CRC Press, New York, NY, 2005. https://doi.org/10.1201/9781420027181.

[25] R.M. Mortier, M.F. Fox, S.T. Orszulik, Chemistry and Technology of Lubricants, Springer Netherlands, Dordrecht, 2010. https://doi.org/10.1007/978-1-4020-8662-5.

[26] ExxonMobil chemical, Group IV Basestocks: Polyalphaolefin Synthetic Basestocks, 2009. https://www.exxonmobilchemical.com/en/products/synthetic-base-stocks (accessed September 13, 2020).

[27] H. Spikes, Friction Modifier Additives, Tribol. Lett. 60 (2015) 1–26. https://doi.org/10.1007/s11249-015-0589-z.

[28] H. Spikes, Friction Modifier Additives, Tribol. Lett. 60 (2015) 5. https://doi.org/10.1007/s11249-015-0589-z.

[29] S. Shahnazar, S. Bagheri, S.B. Abd Hamid, Enhancing lubricant properties by nanoparticle additives, Int. J. Hydrogen Energy. 41 (2016) 3153–3170. https://doi.org/10.1016/j.ijhydene.2015.12.040.

[30] W. Dai, B. Kheireddin, H. Gao, H. Liang, Roles of nanoparticles in oil lubrication, Tribol. Int. 102 (2016) 88–98. https://doi.org/10.1016/j.triboint.2016.05.020.

[31] C. Gao, Y. Wang, D. Hu, Z. Pan, L. Xiang, Tribological properties of magnetite nanoparticles with various morphologies as lubricating additives, J. Nanoparticle Res. 15 (2013) 1502. https://doi.org/10.1007/s11051-013-1502-z.

[32] Y. Choi, C. Lee, Y. Hwang, M. Park, J. Lee, C. Choi, M. Jung, Tribological behavior of copper nanoparticles as additives in oil, Curr. Appl. Phys. 9 (2009) e124–e127. https://doi.org/10.1016/j.cap.2008.12.050.

[33] J. Padgurskas, R. Rukuiza, I. Prosyčevas, R. Kreivaitis, Tribological properties of lubricant additives of Fe, Cu and Co nanoparticles, Tribol. Int. 60 (2013) 224–232.

https://doi.org/10.1016/j.triboint.2012.10.024.

[34] V. Zin, F. Agresti, S. Barison, L. Colla, M. Fabrizio, Influence of Cu, TiO₂ Nanoparticles and Carbon Nano-Horns on Tribological Properties of Engine Oil, J. Nanosci. Nanotechnol. 15 (2015) 3590–3598. https://doi.org/10.1166/jnn.2015.9839.

[35] Y. Zhang, Y. Xu, Y. Yang, S. Zhang, P. Zhang, Z. Zhang, Synthesis and tribological properties of oil-soluble copper nanoparticles as environmentally friendly lubricating oil additives, Ind. Lubr. Tribol. 67 (2015) 227–232. https://doi.org/10.1108/ILT-10-2012-0098.

[36] S. Qiu, Z. Zhou, J. Dong, G. Chen, Preparation of Ni Nanoparticles and Evaluation of Their Tribological Performance as Potential Additives in Oils, J. Tribol. 123 (2001) 441–443. https://doi.org/10.1115/1.1286152.

[37] R. Chou, A.H. Battez, J.J. Cabello, J.L. Viesca, A. Osorio, A. Sagastume, Tribological behavior of polyalphaolefin with the addition of nickel nanoparticles, Tribol. Int. 43 (2010) 2327–2332. https://doi.org/10.1016/j.triboint.2010.08.006.

[38] D.X. Peng, Y. Kang, S.K. Chen, Y.P. Chang, Dispersion and tribological properties of liquid paraffin with added aluminum nanoparticles, Ind. Lubr. Tribol. 62 (2010) 341–348. https://doi.org/10.1108/00368791011076236.

[39] V. Le, J.-W. Lin, Tribological Properties of Aluminum Nanoparticles as Additives in an Aqueous Glycerol Solution, Appl. Sci. 7 (2017) 80. https://doi.org/10.3390/app7010080.

[40] L. Kolodziejczyk, D. Martínez-Martínez, T.C. Rojas, A. Fernández, J.C. Sánchez-López, Surface-modified Pd nanoparticles as a superior additive for lubrication, J. Nanoparticle Res. 9 (2007) 639–645. https://doi.org/10.1007/s11051-006-9124-3.

[41] M.D. Abad, J.C. Sánchez-López, Tribological properties of surface-modified Pd nanoparticles for electrical contacts, Wear. 297 (2013) 943–951. https://doi.org/10.1016/j.wear.2012.11.009.

[42] T. Maliar, S. Achanta, H. Cesiulis, D. Drees, Tribological behaviour of mineral and rapeseed oils containing iron particles, Ind. Lubr. Tribol. 67 (2015) 308–314. https://doi.org/10.1108/ILT-05-2013-0058.

[43] Y.Y. Wu, W.C. Tsui, T.C. Liu, Experimental analysis of tribological properties of lubricating oils with nanoparticle additives, Wear. 262 (2007) 819–825. https://doi.org/10.1016/j.wear.2006.08.021.

[44] M.V. Thottackkad, R.K. Perikinalil, P.N. Kumarapillai, Experimental evaluation on the tribological properties of coconut oil by the addition of CuO nanoparticles, Int. J. Precis. Eng. Manuf. 13 (2012) 111–116. https://doi.org/10.1007/s12541-012-0015-5.

[45] M. Asrul, N.W.M. Zulkifli, H.H. Masjuki, M.A. Kalam, Tribological Properties and Lubricant Mechanism of Nanoparticle in Engine Oil, Procedia Eng. 68 (2013) 320–325. https://doi.org/10.1016/j.proeng.2013.12.186.

[46] S.M. Alves, B.S. Barros, M.F. Trajano, K.S.B. Ribeiro, E. Moura, Tribological behavior of vegetable oil-based lubricants with nanoparticles of oxides in boundary lubrication conditions, Tribol. Int. 65 (2013) 28–36. https://doi.org/10.1016/j.triboint.2013.03.027.

[47] M. Gulzar, H. Masjuki, M. Varman, M. Kalam, R.A. Mufti, N. Zulkifli, R. Yunus, R. Zahid, Improving the AW/EP ability of chemically modified palm oil by adding CuO and MoS2 nanoparticles, Tribol. Int. 88 (2015) 271–279. https://doi.org/10.1016/j.triboint.2015.03.035.

[48] L. Peña-Parás, J. Taha-Tijerina, L. Garza, D. Maldonado-Cortés, R. Michalczewski, C. Lapray, Effect of CuO and Al2O3 nanoparticle additives on the tribological behavior of fully formulated oils, Wear. 332–333 (2015) 1256–1261. https://doi.org/10.1016/j.wear.2015.02.038.

[49] V.S. Jatti, T.P. Singh, Copper oxide nano-particles as friction-reduction and anti-wear additives in lubricating oil, J. Mech. Sci. Technol. 29 (2015) 793–798. https://doi.org/10.1007/s12206-015-0141-y.

[50] A. Hernandez Battez, J.E. Fernandez Rico, A. Navas Arias, J.L. Viesca Rodriguez, R. Chou Rodriguez, J.M. Diaz Fernandez, The tribological behaviour of ZnO nanoparticles as an additive to PAO6, Wear. 261 (2006) 256–263. https://doi.org/10.1016/j.wear.2005.10.001.

[51] X. Ran, X. Yu, Q. Zou, Effect of Particle Concentration on Tribological Properties

of ZnO Nanofluids, Tribol. Trans. 60 (2017) 154–158. https://doi.org/10.1080/10402004.2016.1154233.

[52] S. Arumugam, G. Sriram, Preliminary Study of Nano- and Microscale TiO2 Additives on Tribological Behavior of Chemically Modified Rapeseed Oil, Tribol. Trans. 56 (2013) 797–805. https://doi.org/10.1080/10402004.2013.792977.

[53] M. Laad, V.K.S. Jatti, Titanium oxide nanoparticles as additives in engine oil, J. King Saud Univ. - Eng. Sci. 30 (2018) 116–122. https://doi.org/10.1016/j.jksues.2016.01.008.

[54] T. Luo, X. Wei, X. Huang, L. Huang, F. Yang, Tribological properties of Al2O3 nanoparticles as lubricating oil additives, Ceram. Int. 40 (2014) 7143–7149. https://doi.org/10.1016/j.ceramint.2013.12.050.

[55] S. Ma, S. Zheng, D. Cao, H. Guo, Anti-wear and friction performance of ZrO2 nanoparticles as lubricant additive, Particuology. 8 (2010) 468–472. https://doi.org/10.1016/j.partic.2009.06.007.

[56] Y.Y. Bao, J.L. Sun, L.H. Kong, Tribological properties and lubricating mechanism of SiO 2 nanoparticles in water-based fluid, IOP Conf. Ser. Mater. Sci. Eng. 182 (2017) 012025. https://doi.org/10.1088/1757-899X/182/1/012025.

[57] S.S. Rawat, A.P. Harsha, A.P. Deepak, Tribological performance of paraffin grease with silica nanoparticles as an additive, Appl. Nanosci. 9 (2019) 305–315. https://doi.org/10.1007/s13204-018-0911-9.

[58] J. Zhao, Y. Huang, Y. He, Y. Shi, Nanolubricant additives: A review, Friction. 9 (2021) 891–917. https://doi.org/10.1007/s40544-020-0450-8.

[59] L. Liu, Z. Fang, A. Gu, Z. Guo, Lubrication effect of the paraffin oil filled with functionalized multiwalled carbon nanotubes for bismaleimide resin, Tribol. Lett. 42 (2011) 59–65. https://doi.org/10.1007/s11249-011-9749-y.

[60] H. Song, Z. Wang, J. Yang, Tribological properties of graphene oxide and carbon spheres as lubricating additives, Appl. Phys. A Mater. Sci. Process. 122 (2016) 1–9. https://doi.org/10.1007/s00339-016-0469-x.

[61] L. Joly-Pottuz, B. Vacher, T. Le Mogne, J.M. Martin, T. Mieno, C.N. He, N.Q. Zhao, The role of nickel in Ni-containing nanotubes and onions as lubricant additives,

Tribol. Lett. 29 (2008) 213–219. https://doi.org/10.1007/s11249-008-9298-1.

[62] Y. Peng, Z. Ni, Tribological properties of stearic acid modified multi-walled carbon nanotubes in water, J. Tribol. 135 (2013) 1–5. https://doi.org/10.1115/1.4007676.

[63] Y.-R. Jeng, Y.-H. Huang, P.-C. Tsai, G.-L. Hwang, Tribological Properties of Carbon Nanocapsule Particles as Lubricant Additive, J. Tribol. 136 (2014) 1–9. https://doi.org/10.1115/1.4027994.

[64] L. Zhang, J. Pu, L. Wang, Q. Xue, Frictional dependence of graphene and carbon nanotube in diamond-like carbon/ionic liquids hybrid films in vacuum, Carbon N. Y. 80 (2014) 734–745. https://doi.org/10.1016/j.carbon.2014.09.022.

[65] J.A.C. Cornelio, P.A. Cuervo, L.M. Hoyos-Palacio, J. Lara-Romero, A. Toro, Tribological properties of carbon nanotubes as lubricant additive in oil and water for a wheel–rail system, J. Mater. Res. Technol. 5 (2016) 68–76. https://doi.org/10.1016/j.jmrt.2015.10.006.

[66] B. Wang, W. Tang, X. Liu, Z. Huang, Synthesis of ionic liquid decorated muti-walled carbon nanotubes as the favorable water-based lubricant additives, Appl. Phys. A Mater. Sci. Process. 123 (2017) 680. https://doi.org/10.1007/s00339-017-1320-8.

[67] Y. Su, Z. Tang, G. Wang, R. Wan, Influence of carbon nanotube on the tribological properties of vegetable-based oil, Adv. Mech. Eng. 10 (2018) 168781401877818. https://doi.org/10.1177/1687814018778188.

[68] R.K. Upadhyay, A. Kumar, Boundary lubrication properties and contact mechanism of carbon/MoS2 based nanolubricants under steel/steel contact, Colloid Interface Sci. Commun. 31 (2019) 100186. https://doi.org/10.1016/j.colcom.2019.100186.

[69] S.S. Rawat, A.P. Harsha, A. Chouhan, O.P. Khatri, Effect of Graphene-Based Nanoadditives on the Tribological and Rheological Performance of Paraffin Grease, J. Mater. Eng. Perform. 29 (2020) 2235–2247. https://doi.org/10.1007/s11665-020-04789-8.

[70] T. Luo, X. Wei, H. Zhao, G. Cai, X. Zheng, Tribology properties of Al2O3/TiO2 nanocomposites as lubricant additives, Ceram. Int. 40 (2014) 10103–10109. https://doi.org/10.1016/j.ceramint.2014.03.181.

[71] M. Yi, C. Zhang, The synthesis of MoS2 particles with different morphologies for tribological applications, Tribol. Int. 116 (2017) 285–294. https://doi.org/10.1016/j.triboint.2017.06.045.

[72] H. Baş, Y.E. Karabacak, Investigation of the Effects of Boron Additives on the Performance of Engine Oil, Tribol. Trans. 57 (2014) 740–748. https://doi.org/10.1080/10402004.2014.909549.

[73] D. Jiao, S. Zheng, Y. Wang, R. Guan, B. Cao, The tribology properties of alumina/silica composite nanoparticles as lubricant additives, Appl. Surf. Sci. 257 (2011) 5720–5725. https://doi.org/10.1016/j.apsusc.2011.01.084.

[74] W. Li, S. Zheng, B. Cao, S. Ma, Friction and wear properties of ZrO2/SiO2 composite nanoparticles, J. Nanoparticle Res. 13 (2011) 2129–2137. https://doi.org/10.1007/s11051-010-9970-x.

[75] C. Zhang, S. Zhang, L. Yu, Z. Zhang, Z. Wu, P. Zhang, Preparation and tribological properties of water-soluble copper/silica nanocomposite as a water-based lubricant additive, Appl. Surf. Sci. 259 (2012) 824–830. https://doi.org/10.1016/j.apsusc.2012.07.132.

[76] Y. Meng, F. Su, Y. Chen, Synthesis of nano-Cu/graphene oxide composites by supercritical CO2-assisted deposition as a novel material for reducing friction and wear, Chem. Eng. J. 281 (2015) 11–19. https://doi.org/10.1016/j.cej.2015.06.073.

[77] B. Wu, H. Song, C. Li, R. Song, T. Zhang, X. Hu, Enhanced tribological properties of diesel engine oil with Nano-Lanthanum hydroxide/reduced graphene oxide composites, Tribol. Int. 141 (2020) 105951. https://doi.org/10.1016/j.triboint.2019.105951.

[78] J. Zhang, Y. Zhang, S. Zhang, L. Yu, P. Zhang, Z. Zhang, Preparation of water-soluble lanthanum fluoride nanoparticles and evaluation of their tribological properties, Tribol. Lett. 52 (2013) 305–314. https://doi.org/10.1007/s11249-013-0215-x.

[79] X. Hou, J. He, L. Yu, Z. Li, Z. Zhang, P. Zhang, Preparation and tribological properties of fluorosilane surface-modified lanthanum trifluoride nanoparticles as additive of fluoro silicone oil, Appl. Surf. Sci. 316 (2014) 515–523.

https://doi.org/10.1016/j.apsusc.2014.07.171.

[80] R.N. Gupta, A. Harsha, Antiwear and extreme pressure performance of castor oil with nano-additives, Proc. Inst. Mech. Eng. Part J J. Eng. Tribol. 232 (2018) 1055–1067. https://doi.org/10.1177/1350650117739159.

[81] L. Rapoport, V. Leshchinsky, I. Lapsker, Y. Volovik, O. Nepomnyashchy, M. Lvovsky, R. Popovitz-Biro, Y. Feldman, R. Tenne, Tribological properties of WS2 nanoparticles under mixed lubrication, Wear. 255 (2003) 785–793. https://doi.org/10.1016/S0043-1648(03)00044-9.

[82] L. Yadgarov, V. Petrone, R. Rosentsveig, Y. Feldman, R. Tenne, A. Senatore, Tribological studies of rhenium doped fullerene-like MoS2 nanoparticles in boundary, mixed and elasto-hydrodynamic lubrication conditions, Wear. 297 (2013) 1103–1110. https://doi.org/10.1016/j.wear.2012.11.084.

[83] C.P. Koshy, P.K. Rajendrakumar, M.V. Thottackkad, Evaluation of the tribological and thermo-physical properties of coconut oil added with MoS 2 nanoparticles at elevated temperatures, Wear. 330–331 (2015) 288–308. https://doi.org/10.1016/j.wear.2014.12.044.

[84] V. Srinivas, R.N. Thakur, A.K. Jain, Antiwear, Antifriction, and Extreme Pressure Properties of Motor Bike Engine Oil Dispersed with Molybdenum Disulfide Nanoparticles, Tribol. Trans. 60 (2017) 12–19. https://doi.org/10.1080/10402004.2016.1142034.

[85] S.S. Rawat, A.P. Harsha, D.P. Agarwal, S. Kumari, O.P. Khatri, Pristine and Alkylated MoS2 Nanosheets for Enhancement of Tribological Performance of Paraffin Grease Under Boundary Lubrication Regime, J. Tribol. 141 (2019) 072102–12. https://doi.org/10.1115/1.4043606.

[86] M. Zhang, X. Wang, X. Fu, Y. Xia, Performance and anti-wear mechanism of CaCO3 nanoparticles as a green additive in poly-alpha-olefin, Tribol. Int. 42 (2009) 1029–1039. https://doi.org/10.1016/j.triboint.2009.02.012.

[87] X. Song, S. Zheng, J. Zhang, W. Li, Q. Chen, B. Cao, Synthesis of monodispersed ZnAl 2O 4 nanoparticles and their tribology properties as lubricant additives, Mater. Res. Bull. 47 (2012) 4305–4310.

https://doi.org/10.1016/j.materresbull.2012.09.013.

[88] M.S. Charoo, M.F. Wani, Tribological properties of h-BN nanoparticles as lubricant additive on cylinder liner and piston ring, Lubr. Sci. 29 (2017) 241–254. https://doi.org/10.1002/ls.1366.

[89] V. Saini, J. Bijwe, S. Seth, S.S.V. Ramakumar, Role of base oils in developing extreme pressure lubricants by exploring nano-PTFE particles, Tribol. Int. 143 (2020) 106071. https://doi.org/10.1016/j.triboint.2019.106071.

[90] A. Hernández Battez, R. González, D. Felgueroso, J.E. Fernández, M. del Rocío Fernández, M.A. García, I. Peñuelas, Wear prevention behaviour of nanoparticle suspension under extreme pressure conditions, Wear. 263 (2007) 1568–1574. https://doi.org/10.1016/j.wear.2007.01.093.

[91] J.L. Viesca, A. Hernández Battez, R. González, R. Chou, J.J. Cabello, Antiwear properties of carbon-coated copper nanoparticles used as an additive to a polyalphaolefin, Tribol. Int. 44 (2011) 829–833. https://doi.org/10.1016/j.triboint.2011.02.006.

[92] N.G. Demas, E. V. Timofeeva, J.L. Routbort, G.R. Fenske, Tribological effects of BN and MOS2 nanoparticles added to polyalphaolefin oil in piston skirt/cylinder liner tests, Tribol. Lett. 47 (2012) 91–102. https://doi.org/10.1115/IJTC2012-61062.

[93] G. Yang, J. Zhang, S. Zhang, L. Yu, P. Zhang, B. Zhu, Preparation of triazine derivatives and evaluation of their tribological properties as lubricant additives in poly-alpha olefin, Tribol. Int. 62 (2013) 163–170. https://doi.org/10.1016/j.triboint.2013.02.024.

[94] M. Zhang, X. Wang, W. Liu, Tribological behavior of LaF3 nanoparticles as additives in poly-alpha-olefin, Ind. Lubr. Tribol. 65 (2013) 226–235. https://doi.org/10.1108/00368791311331202.

[95] N. Nunn, Z. Mahbooba, M.G. Ivanov, D.M. Ivanov, D.W. Brenner, O. Shenderova, Tribological properties of polyalphaolefin oil modified with nanocarbon additives, Diam. Relat. Mater. 54 (2015) 97–102. https://doi.org/10.1016/j.diamond.2014.09.003.

[96] T. Sui, B. Song, Y.H. Wen, F. Zhang, Bifunctional hairy silica nanoparticles as high-

performance additives for lubricant, Sci. Rep. 6 (2016) 22696. https://doi.org/10.1038/srep22696.

[97] S.S.N. Azman, N.W.M. Zulkifli, H. Masjuki, M. Gulzar, R. Zahid, Study of tribological properties of lubricating oil blend added with graphene nanoplatelets, J. Mater. Res. 31 (2016) 1932–1938. https://doi.org/10.1557/jmr.2016.24.

[98] J.-M. Huang, H.-D. Qi, R.-B. Gao, G.-J. Zhang, C.-X. Zhang, S.-Z. Yi, Tribological properties of 2 novel Mo/B-based lubricant additives in polyalphaolefin, Lubr. Sci. 29 (2017) 475–484. https://doi.org/10.1002/ls.1381.

[99] A. Zuin, T. Cousseau, A. Sinatora, S.H. Toma, K. Araki, H.E. Toma, Lipophilic magnetite nanoparticles coated with stearic acid: A potential agent for friction and wear reduction, Tribol. Int. 112 (2017) 10–19. https://doi.org/10.1016/j.triboint.2017.03.028.

[100] C. Kumara, D.N. Leonard, H.M. Meyer, H. Luo, B.L. Armstrong, J. Qu, Palladium Nanoparticle-Enabled Ultrathick Tribofilm with Unique Composition, ACS Appl. Mater. Interfaces. 10 (2018) 31804–31812. https://doi.org/10.1021/acsami.8b11213.

[101] J.M. Liñeira del Río, E.R. López, J. Fernández, F. García, Tribological properties of dispersions based on reduced graphene oxide sheets and trimethylolpropane trioleate or PAO 40 oils, J. Mol. Liq. 274 (2019) 568–576. https://doi.org/10.1016/j.molliq.2018.10.107.

[102] S. Wang, D. Chen, Y. Chen, K. Zhu, Dispersion stability and tribological properties of additives introduced by ultrasonic and microwave assisted ball milling in oil, RSC Adv. 10 (2020) 25177–25185. https://doi.org/10.1039/d0ra03414b.

[103] A.V. Bondarev, A. Fraile, T. Polcar, D.V. Shtansky, Mechanisms of friction and wear reduction by h-BN nanosheet and spherical W nanoparticle additives to base oil: Experimental study and molecular dynamics simulation, Tribol. Int. 151 (2020) 106493. https://doi.org/10.1016/j.triboint.2020.106493.

[104] M. Akbulut, Nanoparticle-Based Lubrication Systems, J. Powder Metall. Min. 01 (2012) 1–3. https://doi.org/10.4172/2168-9806.1000e101.

[105] V. Narayanunni, B.A. Kheireddin, M. Akbulut, Influence of surface topography on frictional properties of Cu surfaces under different lubrication conditions:

Comparison of dry, base oil, and ZnS nanowire-based lubrication system, Tribol. Int. 44 (2011) 1720–1725. https://doi.org/10.1016/j.triboint.2011.06.020.

[106] Deepika, Nanotechnology implications for high performance lubricants, SN Appl. Sci. 2 (2020). https://doi.org/10.1007/s42452-020-2916-8.

[107] A. Raina, M. Irfan Ul Haq, A. Anand, J. Sudhanraj, Lubrication Characteristics of Oils Containing Nanoadditives: Influencing Parameters, Market Scenario and Advancements, J. Inst. Eng. Ser. D. (2021). https://doi.org/10.1007/s40033-021-00272-3.

[108] M. Gulzar, H.H. Masjuki, M.A. Kalam, M. Varman, N.W.M. Zulkifli, R.A. Mufti, R. Zahid, Tribological performance of nanoparticles as lubricating oil additives, J. Nanoparticle Res. 18 (2016). https://doi.org/10.1007/s11051-016-3537-4.

[109] S.M. Muzakkir, K.P. Lijesh, H. Hirani, Influence of surfactants on tribological behaviors of MWCNTs (multi-walled carbon nano-tubes), Tribol. - Mater. Surfaces Interfaces. 10 (2016) 74–81. https://doi.org/10.1080/17515831.2016.1138636.

[110] A. Morshed, H. Wu, Z. Jiang, A Comprehensive Review of Water-Based Nanolubricants, Lubricants. 9 (2021) 89. https://doi.org/10.3390/lubricants9090089.

[111] V. Saini, J. Bijwe, S. Seth, S.S.V. Ramakumar, Interfacial interaction of PTFE sub-micron particles in oil with steel surfaces as excellent extreme-pressure additive, J. Mol. Liq. 325 (2021) 115238. https://doi.org/10.1016/j.molliq.2020.115238.

[112] A.A. Thakre, A. Thakur, Study of behaviour of aluminium oxide nanoparticles suspended in SAE20W40 oil under extreme pressure lubrication, Ind. Lubr. Tribol. 67 (2015) 328–335. https://doi.org/10.1108/ILT-06-2014-0057.

[113] H. Schultheiss, T. Tobie, K. Stahl, The Effect of Selected Grease Components on the Wear Behavior of Grease-Lubricated Gears, J. Tribol. 138 (2016) 1–9. https://doi.org/10.1115/1.4031278.

[114] J. Shu, K. Harris, B. Munavirov, R. Westbroek, J. Leckner, S. Glavatskih, Tribology of polypropylene and Li-complex greases with ZDDP and MoDTC additives, Tribol. Int. 118 (2018) 189–195. https://doi.org/10.1016/j.triboint.2017.09.028.

[115] Z. Wang, Y. Xia, Z. Liu, T. Hu, Friction and Wear Behaviour of Laser-Textured Surfaces under the Lubrication of Polyurea Grease Containing Various Additives,

Proc. Inst. Mech. Eng. Part J J. Eng. Tribol. 225 (2011) 139–150. https://doi.org/10.1177/2041305X10394419.

[116] X. Ji, Y. Chen, G. Zhao, X. Wang, W. Liu, Tribological Properties of CaCO3 Nanoparticles as an Additive in Lithium Grease, Tribol. Lett. 41 (2011) 113–119. https://doi.org/10.1007/s11249-010-9688-z.

[117] T. Chen, Y. Xia, Z. Liu, Z. Wang, Preparation and tribological properties of attapulgite – bentonite clay base grease, Ind. Lubr. Tribol. 66 (2014) 538–544. https://doi.org/10.1108/ILT-07-2012-0062.

[118] L. Huang, D. Guo, P.M. Cann, G.T.Y. Wan, S. Wen, Thermal Oxidation Mechanism of Polyalphaolefin Greases with Lithium Soap and Diurea Thickeners: Effects of the Thickener, Tribol. Trans. 59 (2016) 801–809. https://doi.org/10.1080/10402004.2015.1106632.

[119] Y. Dai, W. Niu, X. Zhang, H. Xu, J. Dong, Tribological Investigation of Layered Zirconium Phosphate in Anhydrous Calcium Grease, Lubricants. 5 (2017) 22. https://doi.org/10.3390/lubricants5030022.

[120] N. Kumar, V. Saini, J. Bijwe, Tribological Investigations of Nano and Micro-sized Graphite Particles as an Additive in Lithium-Based Grease, Tribol. Lett. 68 (2020) 1–13. https://doi.org/10.1007/s11249-020-01362-1.

[121] C. Wu, R. Xiong, J. Ni, L. Yao, L. Chen, X. Li, Effects of CuO nanoparticles on friction and vibration behaviors of grease on rolling bearing, Tribol. Int. 152 (2020) 106552. https://doi.org/10.1016/j.triboint.2020.106552.

[122] A. D4172-94, Standard Test Method for Wear Preventive Characteristics of Lubricating Fluid (Four- Ball Method), Annu. B. ASTM Stand. 94 (2016) 1–5. https://doi.org/10.1520/D4172-94R16.2.

[123] A. D2783-03, Standard Test Method for Measurement of Extreme-Pressure Properties of Lubricating Fluids (Four-Ball Method), in: Annu. B. ASTM Stand., 2015: pp. 1–8. https://doi.org/10.1520/D2783- 03R14.

[124] D. Hamrock, B.J. and Dowson, Minimum film thickness in elliptical contacts for different regimes of fluid-film lubrication, NASA Tech. Pap. (1978) 1–22.

[125] B.J. Hamrock, S.R. Schmid, B.O. Jacobson, Fundamental of Fluid Film Lubrication,

in: Marcel Dekker, Inc., New York, 2004.

[126] M.. Saravanan, S.. Babu, K. Sivaprasad, M. Jagannatham, Techno-economics of carbon nanotubes produced by open air arc discharge method, Int. J. Eng. Sci. Technol. 2 (2010) 100–108. https://doi.org/10.4314/ijest.v2i5.60128.

[127] R. Sharma, A.K. Sharma, V. Sharma, Synthesis of carbon nanotubes by arc-discharge and chemical vapor deposition method with analysis of its morphology, dispersion and functionalization characteristics, Cogent Eng. 2 (2015) 1094017. https://doi.org/10.1080/23311916.2015.1094017.

[128] V.T. Le, C.L. Ngo, Q.T. Le, T.T. Ngo, D.N. Nguyen, M.T. Vu, Surface modification and functionalization of carbon nanotube with some organic compounds, Adv. Nat. Sci. Nanosci. Nanotechnol. 4 (2013) 035017. https://doi.org/10.1088/2043-6262/4/3/035017.

[129] Y. Peng, Y. Hu, H. Wang, Tribological behaviors of surfactant-functionalized carbon nanotubes as lubricant additive in water, Tribol. Lett. 25 (2007) 247–253. https://doi.org/10.1007/s11249-006-9176-7.

[130] B. Wang, X. Wang, W. Lou, J. Hao, Rheological and tribological properties of ionic liquid-based nanofluids containing functionalized multi-walled carbon nanotubes, J. Phys. Chem. C. 114 (2010) 8749–8754. https://doi.org/10.1021/jp1005346.

[131] N.M. Vesali, A.A. Khodadadi, Y. Mortazavi, A.O. Sahraei, F. Pourfayaz, M.S. Sedghi, Functionalization of carbon nanotubes using nitric acid oxidation and DBD plasma, World Acad. Sci. Eng. Technol. 37 (2009) 177–179.

[132] T. Sui, B. Song, F. Zhang, Q. Yang, Effects of functional groups on the tribological properties of hairy silica nanoparticles as an additive to polyalphaolefin, RSC Adv. 6 (2015) 393–402. https://doi.org/10.1039/c5ra22932d.

[133] A. Kashyap, A. Harsha, Tribological studies on chemically modified rapeseed oil with CuO and CeO 2 nanoparticles, Proc. Inst. Mech. Eng. Part J J. Eng. Tribol. 230 (2016) 1562–1571. https://doi.org/10.1177/1350650116641328.

[134] R.N. Gupta, A.P. Harsha, Friction and Wear of Nanoadditive-Based Biolubricants in Steel–Steel Sliding Contacts: A Comparative Study, J. Mater. Eng. Perform. 27 (2018) 648–658. https://doi.org/10.1007/s11665-018-3175-3.

[135] L. Zhang, J. Pu, L. Wang, Q. Xue, Frictional dependence of graphene and carbon nanotube in diamond-like carbon/ionic liquids hybrid films in vacuum, Carbon N. Y. 80 (2014) 734–745. https://doi.org/10.1016/j.carbon.2014.09.022.

[136] L. Zhang, J. Pu, L. Wang, Q. Xue, Synergistic Effect of Hybrid Carbon Nanotube–Graphene Oxide as Nanoadditive Enhancing the Frictional Properties of Ionic Liquids in High Vacuum, ACS Appl. Mater. Interfaces. 7 (2015) 8592–8600. https://doi.org/10.1021/acsami.5b00598.

[137] N. Nunn, Z. Mahbooba, M.G. Ivanov, D.M. Ivanov, D.W. Brenner, O. Shenderova, Tribological properties of polyalphaolefin oil modified with nanocarbon additives, Diam. Relat. Mater. 54 (2015) 97–102. https://doi.org/10.1016/j.diamond.2014.09.003.

[138] J. Kogovšek, M. Kalin, Various MoS2-, WS2- and C-Based Micro- and Nanoparticles in Boundary Lubrication, Tribol. Lett. 53 (2014) 585–597. https://doi.org/10.1007/s11249-014-0296-1.

[139] M.Y. Cheah, H.C. Ong, N.W.M. Zulkifli, H.H. Masjuki, A. Salleh, Physicochemical and tribological properties of microalgae oil as biolubricant for hydrogen-powered engine, Int. J. Hydrogen Energy. 45 (2020) 22364–22381. https://doi.org/10.1016/j.ijhydene.2019.11.020.

[140] R. Wäsche, M. Hartelt, V.D. Hodoroaba, Analysis of Nanoscale Wear Particles from Lubricated Steel-Steel Contacts, Tribol. Lett. 58 (2015) 1–10. https://doi.org/10.1007/s11249-015-0534-1.

[141] L. Hongtao, J. Hongmin, H. Haiping, H. Younes, Tribological properties of carbon nanotube grease, Ind. Lubr. Tribol. 66 (2014) 579–583. https://doi.org/10.1108/ILT-08-2012-0071.

[142] R. Kumar, S. Kumar, B. Prakash, A. Sethuramiah, Assessment of engine liner wear from bearing area curves, Wear. 239 (2000) 282–286. https://doi.org/10.1016/S0043-1648(00)00331-8.

[143] M. Sedlaček, B. Podgornik, J. Vižintin, Influence of surface preparation on roughness parameters, friction and wear, Wear. 266 (2009) 482–487. https://doi.org/10.1016/j.wear.2008.04.017.

[144] G. Liu, X. Li, B. Qin, D. Xing, Y. Guo, R. Fan, Investigation of the mending effect and mechanism of copper nano-particles on a tribologically stressed surface, Tribol. Lett. 17 (2004) 961–966. https://doi.org/10.1007/s11249-004-8109-6.

[145] K. Vyavhare, P.B. Aswath, Tribological Properties of Novel Multi-Walled Carbon Nanotubes and Phosphorus Containing Ionic Liquid Hybrids in Grease, Front. Mech. Eng. 5 (2019) 1–18. https://doi.org/10.3389/fmech.2019.00015.

[146] B.S. Ajay Vardhaman, M. Amarnath, J. Ramkumar, P.K. Rai, Experimental Investigations to Enhance the Tribological Performance of Engine Oil by Using Nano-Boric Acid and Functionalized Multiwalled Carbon Nanotubes: A Comparative Study to Assess Wear in Bronze Alloy, J. Mater. Eng. Perform. 27 (2018) 2782–2795. https://doi.org/10.1007/s11665-018-3384-9.

[147] A. Fujimoto, Y. Yamada, M. Koinuma, S. Sato, Origins of sp3C peaks in C1s X-ray Photoelectron Spectra of Carbon Materials, Anal. Chem. 88 (2016) 6110–6114. https://doi.org/10.1021/acs.analchem.6b01327.

[148] K. Gong, X. Wu, G. Zhao, X. Wang, Tribological properties of polymeric aryl phosphates grafted onto multi-walled carbon nanotubes as high-performances lubricant additive, Tribol. Int. 116 (2017) 172–179. https://doi.org/10.1016/j.triboint.2017.07.010.

[149] B. Yu, Z. Liu, C. Ma, J. Sun, W. Liu, F. Zhou, Ionic liquid modified multi-walled carbon nanotubes as lubricant additive, Tribol. Int. 81 (2015) 38–42. https://doi.org/10.1016/j.triboint.2014.07.019.

[150] M.-D. Avilés, V.D. Cao, C. Sánchez, J. Arias-Pardilla, F.-J. Carrión-Vilches, J. Sanes, A.-L. Kjøniksen, M.-D. Bermúdez, R. Pamies, Effect of temperature on the rheological behavior of a new aqueous liquid crystal bio-lubricant, J. Mol. Liq. 301 (2020) 112406. https://doi.org/10.1016/j.molliq.2019.112406.

[151] O. Afzal, W.K. Shafi, M.S. Charoo, Effect of h-BN nanoparticles on the tribological and rheological properties of API-Group I Oils, Energy Sources, Part A Recover. Util. Environ. Eff. 00 (2020) 1–17. https://doi.org/10.1080/15567036.2020.1864516.

[152] D. Kim, L.A. Archer, Nanoscale organic-inorganic hybrid lubricants, Langmuir. 27

(2011) 3083–3094. https://doi.org/10.1021/la104937t.

[153] B.P. Chang, W.H. Chan, M.H. Zamri, H. Md Akil, H.G. Chuah, Investigating the Effects of Operational Factors on Wear Properties of Heat-Treated Pultruded Kenaf Fiber-Reinforced Polyester Composites using Taguchi Method, J. Nat. Fibers. 16 (2019) 702–717. https://doi.org/10.1080/15440478.2018.1432001.

[154] D.X. Peng, Y. Kang, Preparation of SiO2 nanoparticles and investigation of its tribological behavior as additive in liquid paraffin, Ind. Lubr. Tribol. 66 (2014) 662–670. https://doi.org/10.1108/ILT-08-2012-0075.

[155] M.S. Phadke, Quality Engineering Using Robust Design.pdf, P T R Prentice Hall Inc., New Jersey, USA, New Jersey, 1995.

[156] A. Roushan, A. Bandyopadhyay, S. Banerjee, Multiple performance characteristics optimisation in side and face milling of glass fibre reinforced polyester composite at different weightage of performances by grey relational analysis, Int. J. Mach. Mach. Mater. 19 (2017) 41–56. https://doi.org/10.1504/IJMMM.2017.081187.

[157] N.F. Azman, S. Samion, Dispersion Stability and Lubrication Mechanism of Nanolubricants: A Review, Int. J. Precis. Eng. Manuf. Technol. 6 (2019) 393–414. https://doi.org/10.1007/s40684-019-00080-x.

[158] M.Y. Cheah, H.C. Ong, N.W.M. Zulkifli, H.H. Masjuki, A. Salleh, Physicochemical and tribological properties of microalgae oil as biolubricant for hydrogen-powered engine, Int. J. Hydrogen Energy. 45 (2020) 22364–22381. https://doi.org/10.1016/j.ijhydene.2019.11.020.

[159] W.A.P.J. Premaratne, W.M.G.I. Priyadarshana, S.H.P. Gunawardena, A.A.P. De Alwis, Synthesis of Nanosilica from Paddy Husk Ash and Their Surface Functionalization, J. Sci. Univ. Kelaniya Sri Lanka. 8 (2014) 33–48. https://doi.org/10.4038/josuk.v8i0.7238.

[160] N.S. Labidi, A. Iddou, Adsorption of Oleic Acid on Quartz /Water Interface, J. Saudi Chem. Soc. 11 (2007) 221–234.

[161] L. Wang, M. Zhang, X. Wang, W. Liu, The preparation of CeF3 nanocluster capped with oleic acid by extraction method and application to lithium grease, Mater. Res. Bull. 43 (2008) 2220–2227. https://doi.org/10.1016/j.materresbull.2007.08.024.

[162] X. Hou, C. Yang, J. He, Z. Li, Z. Zhang, Preparation and tribological properties of lanthanum trifluoride nanoparticles-decorated graphene oxide nanosheets, Ind. Eng. Chem. Res. 54 (2015) 4773–4780. https://doi.org/10.1021/acs.iecr.5b00576.

[163] Y. He, L. Wang, X. Wang, C. Shen, Q. Hu, A. Zhou, X. Liu, Surface reformation of 2D MXene by in situ LaF3-decorated and enhancement of energy storage in lithium-ion batteries, J. Mater. Sci. Mater. Electron. 31 (2020) 6735–6743. https://doi.org/10.1007/s10854-020-03230-z.

[164] C.E. Secu, E. Matei, C. Negrila, M. Secu, The influence of the nanocrystals size and surface on the Yb/Er doped LaF3 luminescence properties, J. Alloys Compd. 791 (2019) 1098–1104. https://doi.org/10.1016/j.jallcom.2019.03.267.

[165] A.A. Yadav, V.C. Lokhande, R.N. Bulakhe, C.D. Lokhande, Amperometric CO2 gas sensor based on interconnected web-like nanoparticles of La2O3 synthesized by ultrasonic spray pyrolysis, Microchim. Acta. 184 (2017) 3713–3720. https://doi.org/10.1007/s00604-017-2364-3.

[166] J.F. Moulder, W.F. Stickle, P.E. Sobol, K.D. Bomben, Handbook of X-ray Photoelectron Spectroscopy Edited by, Minnesota, USA, 1993. https://books.google.com/books/about/Handbook_of_X_ray_Photoelectron_Spectros.html?hl=fr&id=A_XGQgAACAAJ.

[167] V. Edachery, S. R, S. V. Kailas, Influence of surface texture directionality and roughness on wettability, sliding angle, contact angle hysteresis, and lubricant entrapment capability, Tribol. Int. 158 (2021) 106932. https://doi.org/10.1016/j.triboint.2021.106932.

[168] M. Sedlaček, B. Podgornik, J. Vižintin, Correlation between standard roughness parameters skewness and kurtosis and tribological behaviour of contact surfaces, Tribol. Int. 48 (2012) 102–112. https://doi.org/10.1016/j.triboint.2011.11.008.

[169] S.S. Rawat, A.P. Harsha, O.P. Khatri, Synergistic effect of binary systems of nanostructured MoS2/SiO2 and GO/SiO2 as additives to coconut oil-derived grease: Enhancement of physicochemical and lubrication properties, Lubr. Sci. 33 (2021) 290–307. https://doi.org/10.1002/ls.1554.

[170] E.S. Gadelmawla, M.M. Koura, T.M.A. Maksoud, I.M. Elewa, H.H. Soliman,

Roughness parameters, J. Mater. Process. Technol. 123 (2002) 133–145. https://doi.org/10.1016/S0924-0136(02)00060-2.

[171] R.A. Waikar, Y.B. Guo, A comprehensive characterization of 3D surface topography induced by hard turning versus grinding, J. Mater. Process. Technol. 197 (2008) 189–199. https://doi.org/10.1016/j.jmatprotec.2007.05.054.

[172] N. Kumar, V. Saini, J. Bijwe, Performance properties of lithium greases with PTFE particles as additive: Controlling parameter- size or shape?, Tribol. Int. 148 (2020) 106302. https://doi.org/10.1016/j.triboint.2020.106302.

[173] S.S. Rawat, A.P. Harsha, S. Das, A.P. Deepak, Effect of CuO and ZnO Nano-Additives on the Tribological Performance of Paraffin Oil–Based Lithium Grease, Tribol. Trans. 63 (2020) 90–100. https://doi.org/10.1080/10402004.2019.1664684.

[174] A. García Tuero, M. Bartolomé, D. Gonçalves, J.L. Viesca, A. Fernández-González, J.H.O. Seabra, A. Hernández Battez, Phosphonium-based ionic liquids as additives in calcium/lithium greases, J. Mol. Liq. 338 (2021) 116697. https://doi.org/10.1016/j.molliq.2021.116697.

[175] G.W. Stachowiak, A.W. Batchelor, ENGINEERING TRIBOLOGY, Butterworth-Heinemann, USA, 2013.

[176] J.L. do Vale, V. de C. Beltrão, C.H. da Silva, G. Pintaúde, Evaluation of the error of the light beam incidence on concave surfaces in 3D roughness parameters using optical interferometry, Meas. J. Int. Meas. Confed. 120 (2018) 182–192. https://doi.org/10.1016/j.measurement.2018.02.022.

[177] K. Gong, X. Wu, G. Zhao, X. Wang, Tribological properties of polymeric aryl phosphates grafted onto multi-walled carbon nanotubes as high-performances lubricant additive, Tribol. Int. 116 (2017) 172–179. https://doi.org/10.1016/j.triboint.2017.07.010.

[178] Z. Zhang, W. Liu, Q. Xue, Study on lubricating mechanisms of La(OH)3 nanocluster modified by compound containing nitrogen in liquid paraffin, Wear. 218 (1998) 139–144. https://doi.org/10.1016/S0043-1648(98)00225-7.

[179] G. Jiang, W. Guan, Q. Zheng, A study on fullerene-acrylamide copolymer nanoball - A new type of water-based lubrication additive, Wear. 258 (2005) 1625–1629.

https://doi.org/10.1016/j.wear.2004.11.016.

Appendix–A

❖ Calculation of maximum contact pressure

The maximum contact pressure (i.e., Hertzian stress, P_{max}) was computed using Eq. (A.1).

$$P_{max} = \frac{3W}{2\pi a^2} \tag{A.1}$$

$$a = \left[\frac{3WR'}{E'}\right]^{1/3} \tag{A.2}$$

$$\frac{1}{E'} = \frac{1}{2}\left[\frac{1-\vartheta_1^2}{E_1} + \frac{1-\vartheta_2^2}{E_2}\right] \tag{A.3}$$

$$\frac{1}{R'} = \frac{1}{R_x} + \frac{1}{R_y} = \frac{1}{R_{1x}} + \frac{1}{R_{2x}} + \frac{1}{R_{1y}} + \frac{1}{R_{2y}} \tag{A.4}$$

Where;

W: Normal load (N),

a: Hertzian radius (i.e., the radius of contact area)

R', R_1 and R_2: Effective radius or reduced radius of curvature, the radius of body 1, body 2, respectively. (The subscripts ‘x’ and ‘y’ refer to x–direction and y–direction)

E_1, E_2 and E': Young’s modulus of body 1, body 2, and reduced Young’s modulus, respectively.

ϑ_1 and ϑ_2: Poisson’s ratio for body 1, body 2, respectively.

❖ Calculation of P_{max} in case of four- ball tribometer

In four- ball tribometer, the tribo-pairs exhibit ball-on-ball type geometry and diameter of both bodies (i.e., steel balls) are identical i.e., 12.7 mm.

Therefore, $R_{1x} = R_{1y} = R_1$ and $R_{2x} = R_{2y} = R_2$

The reduced radius of curvature can be calculated as

$$\frac{1}{R'} = 2\left[\frac{1}{R_1} + \frac{1}{R_2}\right]$$

$$\frac{1}{R'} = 2\left[\frac{1}{6.35 \times 10^{-3}} + \frac{1}{6.35 \times 10^{-3}}\right]$$

$$R' = 1.58 \times 10^{-3} \text{ m} \tag{A.5}$$

Since the material properties of both bodies are the same. Therefore,

$E_1 = E_2 = 210 \times 10^9$ Pa and $\vartheta_1 = \vartheta_2 = 0.3$

The reduced Young's modulus can be calculated by using Eq. (A.3)

$$\frac{1}{E'} = \frac{1}{2}\left[\frac{1 - 0.3^2}{210 \times 10^9} + \frac{1 - 0.3^2}{210 \times 10^9}\right]$$

$$E' = 2.31 \times 10^{11} \text{ Pa} \tag{A.6}$$

In the anti-wear test, the contact angles between balls were 35.265° as per ASTM standard. The applied load was 40 kgf (or 392 N), and Eq. (A.7) was used to calculate the actual contact load.

$$P = N \cos(35.265^{\circ}) \tag{A.7}$$

Where;

P: applied load (392 N)

N: total actual contact load on three lower balls.

One-third of the total contact load “N” has been uniformly distributed among three lower balls (i.e., W = N/3).

Therefore, normal load on one ball

$$W = 0.40825P \; = \; 0.40825 \times 392$$

$$W = 160.03 \text{ N} \tag{A.8}$$

Hertzian radius or radius of contact area was calculated by using Eq. (A.2)

$$a = \left[\frac{3 \times 160.03 \times 1.58 \times 10^{-3}}{2.31 \times 10^{11}}\right]^{1/3}$$

$$a = 1.49 \times 10^{-4} \text{ m} \tag{A.9}$$

The maximum contact pressure or Hertz stress as per Eq. (A.1)

$$P_{max} = \frac{3 \times 160.03}{2 \times 3.14 \times (1.49 \times 10^{-4})^2}$$

$$P_{max} = 3.443 \times 10^9 \text{ Pa}$$

$$P_{max} = 3.4 \text{ GPa} \tag{A.10}$$

❖ Calculation of maximum contact pressure for SRV 5 tribometer

In SRV 5 tribo-testing, the ball-on disc-type configuration, confirming the point contact between the mating surfaces, and the contact area is also circular. Therefore, the radius of contact area can be determined by using Eq. (A.2) as follows:

$$a = \left[\frac{3WR'}{E'}\right]^{1/3}$$

In ball-on-disc type geometry, for the ball (body 1): $R_{1x} = R_{1y} = R_1$ and for disc (body 2): $R_{2x} = R_{2y} = \infty$

Therefore, the effective radius of curvature can be calculated as per Eq. (A4), as follows:

$$\frac{1}{R'} = \frac{2}{R_1} = \frac{2}{5 \times 10^{-3}}$$

$$R' = 2.5 \times 10^{-3} \text{ m} \tag{A.11}$$

Since both mating bodies (i.e., ball and disc) are made of the same material (AISI 52100). Therefore, $E_1 = E_2 = 210 \times 10^9$ Pa and $\vartheta_1 = \vartheta_2 = 0.3$

The reduced Young's modulus was calculated by using Eq. (A.3), as

$$\frac{1}{E'} = \frac{1}{2}\left[\frac{1 - 0.3^2}{210 \times 10^9} + \frac{1 - 0.3^2}{210 \times 10^9}\right]$$

$$E' = 2.31 \times 10^{11} \text{ Pa} \tag{A.12}$$

The radius of contact area or Hertzian radius

$$a = \left[\frac{3 \times W \times 2.5 \times 10^{-3}}{2.31 \times 10^{11}}\right]^{1/3}$$

$$a = 3.19 \times 10^{-4} \times W^{1/3} \tag{A.13}$$

The Hertzian radius at different applied load was calculated and are summarized in Table A.1.

Therefore, Maximum contact pressure or Hertzian contact stress

$$P_{max} = \frac{3 \times W}{2 \times 3.14 \times (a)^2}$$

$$P_{max} = 0.4777 \times \frac{W}{a^2} \tag{A.14}$$

The Hertzian contact stress under different applied load was determined and are summarized in Table A.1.

Table A.1: Summary of calculated Hertzian radius and Hertzian contact stress under different loading conditions

Applied normal load (N)	**Hertzian radius ($\times\ 10^{-4}$; m)**	**Hertzian contact stress (P_{max}; GPa)**
50	1.18	1.73
200	1.87	2.74
300	2.14	3.14

❖ Calculation of maximum contact pressure in case of ball-on-disc tribometer

In ball-on-disc tribometer, body 1, i.e., steel ball, has a diameter of 10 mm and is made of high chrome steel (AISI 52100). Therefore, $E_1 = 210 \times 10^9$ Pa and $\vartheta_1 = 0.3$. Body 2 is the disc which is made of hardened steel (EN 31). Thus, $E_2 = 200 \times 10^9$ Pa and $\vartheta_2 = 0.3$.

The calculated effective radius of curvature using Eq. (A.4) is

$$R' = 2.5 \times 10^{-3} \text{ m} \tag{A.15}$$

The reduced Young's modulus was calculated by using Eq. (A.3)

$$E' = 2.25 \times 10^{11} \text{ Pa} \tag{A.16}$$

The radius of contact area or Hertzian radius and maximum contact pressure or Hertzian contact stress was computed as per Eq. (A.2) and, summarized in Table A.2.

Table A.2: Summary of calculated Hertzian radius and Hertzian contact stress under different loading conditions

Applied normal load (N)	**Hertzian radius ($\times\ 10^{-4}$; m)**	**Hertzian contact stress (P_{max}; GPa)**
50	1.19	1.7
80	1.39	1.99
100	1.49	2.14

Appendix– B

❖ Calculation of mean wear volume of worn surface in case of four-ball tribometer

The wear scar diameter of the three stationary steel balls was considered to ascertain the wear of balls. The mean wear volume (MWV) was computed by using Eq. (B.1)

$$MWV = \frac{\pi d_0^4}{64R'}\left\{\left(\frac{d_m}{d_0}\right)^4 - \left(\frac{d_m}{d_0}\right)\right\} \tag{B.1}$$

Where, d_m: mean wear scar diameter (WSD)

$$d_m = (d_1 + d_2 + d_3)/3 \tag{B.2}$$

d_1, d_2 and d_3: mean scar diameter of stationary ball 1, ball 2 and ball 3

$$d_0 = \text{Hertzian diameter} = 2a = 2\left[\frac{3WR'}{E\prime}\right]^{1/3} \tag{B.3}$$

Hertzian radius or radius of contact area (calculation procedure in provided in Appendix-A)

$$a = 1.49 \times 10^{-4}\ \text{m}$$

The diameter of contact area or Hertzian diameter,

$$d_0 = 2a = 2 \times 1.49 \times 10^{-4}\ \text{m}$$

$$d_0 = 2.98 \times 10^{-4}\ \text{m} \tag{B.4}$$

The reduced Young's modulus was calculated as per Appendix-A

$$E' = 2.31 \times 10^{11}\ \text{Pa} \tag{B.5}$$

The reduced radius of curvature (calculation procedure is given in Appendix-A)

$$R' = 1.58 \times 10^{-3} \text{ m} \tag{B.6}$$

The mean WSD of three stationary steel balls lubricated with plain PAO 4 were 1086.2 µm, 1077.6 µm, and 1042.1 µm. Therefore, the mean WSD of three stationary steel balls

$$d_m = (1086.2 + 1077.6 + 1043.1)/3$$

$$d_m = 1068.9 \text{ µm}$$

$$d_m = 1068.9 \times 10^{-6} \text{ m} \tag{B.7}$$

The mean wear volume of worn surfaces of steel ball

$$MWV = \frac{3.14 \times \ (2.98 \times 10^{-4})^4}{64 \times 1.58 \times 10^{-3}} \left\{ \left(\frac{1068.9 \times 10^{-6}}{2.98 \times 10^{-4}} \right)^4 - \left(\frac{1068.9 \times 10^{-6}}{2.98 \times 10^{-4}} \right) \right\}$$

$$MWV = 1.97 \times 10^{-11} \text{ m}^3$$

$$MWV = 197 \times 10^{-4} \text{ mm}^3$$

Similarly, the mean wear volume of each worn surfaces of steel balls lubricated with various lubricant formulation were calculated.

❖ Calculation of mean wear volume of worn surface in case of SRV 5 tribometer

The wear volume (WV) was estimated by considering the total volume loss of both mating pairs (i.e., ball and disc) as per Eq. (B.8). Equations (B.9) -(B.13) are the auxiliary equations to Eq. (B.8)

$$WV = WV_{ball} + WV_{disc} \tag{B.8}$$

$$WV_{ball} = \left(\frac{\pi W_{L_1} d_2^2}{8} \right) \tag{B.9}$$

Where;

$$W_{L_1} = \left[R_1 - \left\{\sqrt{\left(R_1^2 - \frac{d_2^2}{4}\right)}\right\}\right] - W_{L_2} \tag{B.10}$$

$$WV_{disc} = \left(\frac{\pi W_{L_2} d_2^2}{8}\right) + \left(\Delta x W_q\right) \tag{B.11}$$

Where;

$$W_{L_2} = \left[R^* - \left\{\sqrt{\left(R^{*2} - \frac{d_2^2}{4}\right)}\right\}\right] \tag{B.12}$$

$$R^* = \frac{d_2^3}{12 W_q} \tag{B.13}$$

Where; WV_{ball} and WV_{disc}: volumetric wear of ball and disc, respectively.

d_2: wear scar diameter perpendicular to the sliding direction.

R_1 : radius of steel ball.

R^*: the approximate radius of wear scar on the disc after the test.

W_q: represent the cross-sectional wear area (planimetric wear) of the disc,

W_{L_1}: linear wear of ball.

W_{L_2}: linear wear of disc.

Δx: the stroke length.

❖ Calculation of mean wear volume of worn surface in case of ball-on-disc tribometer

In the "ball on disc" type of arrangement, the specific wear rate was calculated by assuming negligible wear of the disc as compared to the ball. The specific wear rate (K) was computed as per Archard's equation and given in Eq. (B.14).

$$K = {}^{V}\!/_{WS} \tag{B.14}$$

Where V is the wear volume of the worn surface of the tested ball (mm^3), W is the applied load (N), and S is the sliding distance (m).

The wear volume was determined geometrically using the diameter and the height of the wear scar as given in Equation (B.15). Eq. (3.16) is the subsidiary equation to Eq. (B.15).

$$V = \pi h^2 \left(R_1 - \frac{h}{3}\right) \tag{B.15}$$

$$h = R_1 - \sqrt{R_1^2 - \left(\frac{d}{2}\right)^2} \tag{B.16}$$

Where; R_1 is the radius of the steel ball (mm).

h: the height of wear scar (mm).

d: diameter of wear scar (mm) of the tested ball.

Appendix– C

❖ Calculation of lubricant minimum film thickness

The minimum film thickness was calculated in accordance with Hamrock and Dowson's equation by assuming hard elastohydrodynamic lubrication, and it is as shown by Eq. (C.1).

$$\frac{h_{\min}}{R'} = 3.63 \left(\frac{u\eta_0}{E'R'}\right)^{0.68} (\xi E')^{0.49} \left(\frac{W}{E'R'^2}\right)^{-0.073} \left(1 - \mathrm{e}^{-0.68k}\right) \tag{C.1}$$

Where;

h_{min}: lubricant minimum film thickness (m);

u: mean velocity (m/s) i.e., $u = \frac{u_1+u_2}{2}$; where, u_1 is the velocity of body 1 and u_2 is the velocity of body 2;

η_0: dynamic viscosity of lubricant (Pa-S);

R': reduced radius of curvature (m);

E': reduced Young's modulus (Pa);

w: normal load (N);

k: elliptical parameter; (*k* =1 for point contact and *k* =0 for line contact)

One of the essential parameters required to compute h_{min} is the pressure viscosity coefficient (ξ), which is assessed with the help of the Wooster equation (Eq. (C.2)).

$$\xi = (0.6 + 0.965 \times log_{10}\eta)10^{-8} \tag{C.2}$$

Where;

ξ: Pressure–viscosity coefficient (m^2/N)

η: the atmospheric viscosity of lubricant (cP)

❖ Calculation of minimum film thickness in case of four-ball tribo-testing

In four-ball tribometer, the tribo-pairs exhibit ball-on-ball type geometry, and the diameter of both bodies (i.e., steel balls) are identical, i.e., 12.7 mm.

Therefore, $R_{1x} = R_{1y} = R_1$ and $R_{2x} = R_{2y} = R_2$

The reduced radius of curvature can be calculated as

$$\frac{1}{R'} = 2\left[\frac{1}{R_1} + \frac{1}{R_2}\right] \tag{C.3}$$

$$\frac{1}{R'} = 2\left[\frac{1}{6.35 \times 10^{-3}} + \frac{1}{6.35 \times 10^{-3}}\right]$$

$$R' = 1.58 \times 10^{-3} \text{ m}$$

Since the material properties of both bodies are the same. Therefore,

$E_1 = E_2 = 210 \times 10^9$ Pa and $\vartheta_1 = \vartheta_2 = 0.3$

The reduced Young's modulus can be calculated by using Eq. (A.3) of Appendix-A

$$\frac{1}{E'} = \frac{1}{2}\left[\frac{1 - 0.3^2}{210 \times 10^9} + \frac{1 - 0.3^2}{210 \times 10^9}\right]$$

$$E' = 2.31 \times 10^{11} \text{ Pa} \tag{C.4}$$

Normal load on one ball

$$W = 0.40825P = 0.40825 \times 392$$

$$W = 160.03 \text{ N} \tag{C.5}$$

The velocity of body 1(i.e., upper rotating steel ball)

$$u_1 = \frac{\pi D N_r}{60}$$

$$u_1 = \frac{3.14 \times 12.7 \times 10^{-3} \times 1200}{60}$$

$$u_1 = 0.7975 \text{ m/s}$$

Bottom balls were fixed, therefore $u_2 = 0$

The mean velocity, $u = \frac{u_1 + u_2}{2}$

$$u = \frac{0.7975 + 0}{2}$$

$$u = 0.3988 \text{ m/s} \qquad \text{(C.6)}$$

In the computation of pressure viscosity coefficient (ξ), the dynamic viscosity of different grades of PAOs was calculated by considering the kinematic viscosity at 40 °C and density, as shown in Table 3.1.

For example,

The dynamic viscosity of PAO 4 = 15.60×10^{-3} Pa-s= 15.6 cP

The pressure viscosity coefficient (ξ) was calculated by using Eq. (C7) as follows

$$\xi = (0.6 + 0.965 \times log_{10}\eta)10^{-8} \qquad \text{(C.7)}$$

For PAO 4 base oil,

$$\xi = (0.6 + 0.965 \times log_{10}15.6)10^{-8}$$

$$\xi = 1.75 \times 10^{-8} \text{ m}^2\text{/N} \qquad \text{(C.8)}$$

The calculated values of ξ for all grades of PAOs is shown in Table C.1.

Now considering Eq. (C.1), the minimum film thickness in case of PAO 4 was determined as follows:

$$\frac{h_{\min}}{R'} = 3.63\left(\frac{u\eta_0}{E'R'}\right)^{0.68}(\xi E')^{0.49}\left(\frac{W}{E'R'^2}\right)^{-0.073}(1-\mathrm{e}^{-0.68k})$$

$$\frac{h_{\min}}{1.58\times10^{-3}} = 3.63\left(\frac{0.39887\times15.6\times\ 10^{-3}}{2.31\times10^{11}\times\ 1.58\times10^{-3}}\right)^{0.68}(1.75\times10^{-8}\times2.31$$

$$\times\,10^{11})^{0.49}\left[\frac{160.03}{2.31\times10^{11}\times(1.58\times10^{-3})^2}\right]^{-0.073}(1-\mathrm{e}^{-0.68})$$

$$\frac{h_{\min}}{1.58\times10^{-3}} = 3.63(1.71\times10^{-11})^{0.68}(4.04\times10^{3})^{0.49}(2.78\times10^{-4})^{-0.073}(0.493383)$$

$$\frac{h_{\min}}{1.58\times10^{-3}} = 9.0832\times10^{-6}$$

$$h_{\min} = 9.0832\times10^{-6}\times1.58\times10^{-3}$$

$$h_{\min} = 14.35\times10^{-9}\ \mathrm{m}$$

$$h_{\min} = 14.36\ \mathrm{nm}$$

To elucidate the lubrication regime, film thickness ratio or lambda ratio (λ) was calculated using Eq. (C.9).

$$\lambda = \frac{h_{min}}{\sigma^*} \tag{C.9}$$

Where; $\sigma^* = \sqrt{(\sigma_1^2+\sigma_2^2)}$ = composite surface roughness

σ_1 and σ_2 are the surface roughness of body 1 and body 2. The surface roughness of body 1 (steel ball) and body 2 (steel ball) is 0.201 µm.

$$\lambda = \frac{14.35\times10^{-9}}{\sqrt{(2.01\times10^{-7})^2+\ (2.01\times10^{-7})^2}}$$

$$\lambda = 0.0504$$

Similarly, the $h_{\min}$ and λ were calculated for all grades of PAOs and summarized in Table C.1.

Table C.1: Summary of calculated pressure viscosity coefficient, minimum film thickness, and film thickness parameter of different PAOs

Base oil	**Pressure viscosity coefficient (ξ), (GPa)$^{-1}$**	**Minimum film thickness ($h_{\min}$), (nm)**	**Film thickness ratio (λ)**
PAO 4	17.5	14.34	0.051
PAO 6	19.6	21.27	0.075
PAO 40	30.4	151.6	0.533
PAO 100	34.9	335.7	1.18

❖ Calculation of minimum film thickness in case of SRV- 5 tribo-testing

In ball-on-disc type geometry, for the ball (body 1): $R_{1x} = R_{1y} = R_1$ and for disc (body 2): $R_{2x} = R_{2y} = \infty$

Therefore, the effective radius of curvature $R' = 2.5 \times 10^{-3}$ m (C.10)

Since both mating bodies (i.e., ball and disc) are made of the same material (AISI 52100).

Therefore, $E_1 = E_2 = 210 \times 10^9$ Pa and $\vartheta_1 = \vartheta_2 = 0.3$

The computed reduced Young's modulus

$$E' = 2.31 \times 10^{11} \text{ Pa}$$

The velocity of body 1(i.e., upper rotating steel ball)

$$u_1 = 0.1 \text{ m/s}$$

Body 2 (i.e., disc) is stationary, therefore $u_2 = 0$

The mean velocity, $$u = \frac{u_1 + u_2}{2}$$

$$u = \frac{0.1 + 0}{2}$$

$$u = 0.05 \text{ m/s} \tag{C.11}$$

The pressure-viscosity coefficient, lubricant minimum film thickness, and film thickness ratio were determined according to the procedure explained in Section 1.1 and summarized in Table C.2.

Table C.2: Summary of calculated pressure viscosity coefficient, minimum film thickness and film thickness parameter for different base oils

Base oil	Pressure viscosity coefficient (ξ), (GPa)$^{-1}$	Minimum film thickness ($h_{\min}$), (nm)	Film thickness ratio (λ)
PAO 4	17.5	4.71	0.114
PAO 6	19.6	6.32	0.153
PAO 100	34.9	96.7	2.35
PPG 2000	28.8	32.9	0.779

❖ Calculation of minimum film thickness in case of Pin-on-disc tribo-testing

In ball-on-disc tribometer, body 1, i.e., steel ball, has a diameter of 10 mm and is made of high chrome steel (AISI 52100). Therefore, $E_1 = 210 \times 10^9$ Pa and $\vartheta_1 = 0.3$. Body 2 is the disc which is made of hardened steel (EN 31). Thus, $E_2 = 200 \times 10^9$ Pa and $\vartheta_2 = 0.3$.

The calculated effective radius of curvature using Eq. (A.4) of Appendix-A is

$$R' = 2.5 \times 10^{-3} \text{ m} \tag{C.12}$$

The reduced Young's modulus was calculated by using Eq. (A.3) of Appendix-A

$$E' = 2.25 \times 10^{11} \text{ Pa} \tag{C.13}$$

Since the velocities of body 1(i.e., upper rotating steel ball) are 0.42 m/s, 1.099 m/s and 1.57 m/s.

Therefore, mean velocities are 0.21 m/s, 0.5495 m/s and 0.785 m/s

The pressure-viscosity coefficient, lubricant minimum film thickness, and film thickness ratio as per L_{18} orthogonal array were determined according to the procedure explained in Section 1.1 and summarized in Table C.3.

Table C.3: Summary of calculated pressure viscosity coefficient, minimum film thickness and film thickness parameter as per L_{18} orthogonal array

Expt. No.	**Velocity, (m/s)**	**Load, (N)**	**Base oil**	**Pressure viscosity coefficient (ξ), $(\mathrm{GPa})^{-1}$**	**Minimum film thickness (h_{min}), (nm)**	**Film thickness ratio, (λ)**
1	0.42	50	PAO 4	17.5	26.6	0.058
2	1.099	80	PAO 6	19.6	69.5	0.152
3	1.57	100	PAO 40	30.4	501.3	1.098
4	0.42	50	PAO 6	19.6	37.4	0.082
5	1.099	80	PAO 40	30.4	399.8	0.876
6	1.57	100	PAO 4	17.5	62.08	0.136
7	1.099	50	PAO 4	17.5	51.2	0.112
8	1.57	80	PAO 6	19.6	88.6	0.194
9	0.42	100	PAO 40	30.4	204.5	0.448
10	1.57	50	PAO 40	30.4	527.3	1.155
11	0.42	80	PAO 4	17.5	25.7	0.056
12	1.099	100	PAO 6	19.6	25.7	0.150
13	1.099	50	PAO 40	30.4	68.4	0.906
14	1.57	80	PAO 4	17.5	413.7	0.138
15	0.42	100	PAO 6	19.6	63.1	0.078
16	1.57	50	PAO 6	19.6	35.5	0.201
17	0.42	80	PAO 40	30.4	91.7	0.455
18	1.099	100	PAO 4	17.5	207.9	0.107

Appendix–D

- **Calculation of the stoichiometric amount of 12–hydroxystearic acid and lithium hydroxide monohydrate required in the formulation of 250 gm grease sample**

The molecular weight of thickener ingredients is listed in Table D.1.

Table D.1: Molecular weight of thickener ingredients

Name of thickner ingredients	Molecular weight (gm/mol)
12–hydroxystearic acid	300.53
Lithium hydroxide monohydrate	41.96
Lithium 12–hydroxystearate	306.40

$$\text{12 − hydroxy stearic acid + lithium hydroxide} \longrightarrow \text{Lithium 12 − hydroxy stearate + water}$$

$$CH_3 - (CH_2)_5 - CHOH - (CH_2)_{10} - COOH + LiOH \longrightarrow CH_3 - (CH_2)_5 - CHOH - (CH_2)_{10} - COOLi + H_2O$$

$$\text{Moles of lithium 12–hydroxystearate in mixture} = \frac{\text{weight of compound}}{\text{molecular weight}}$$

$$= \frac{35\ \text{gm}}{306.40\ \text{gm/mole}}$$

$$= 0.1142\ \text{mole}$$

Weight of 12–hydroxystearic acid required = number of moles × molecular weight

= 0.1142 × 300.53 = 34.32 gm

Weight of lithium hydroxide monohydrate required = number of moles × molecular weight

= 0.1142 × 41.96 = 4.79 gm

Appendix–E

Copyright permissions

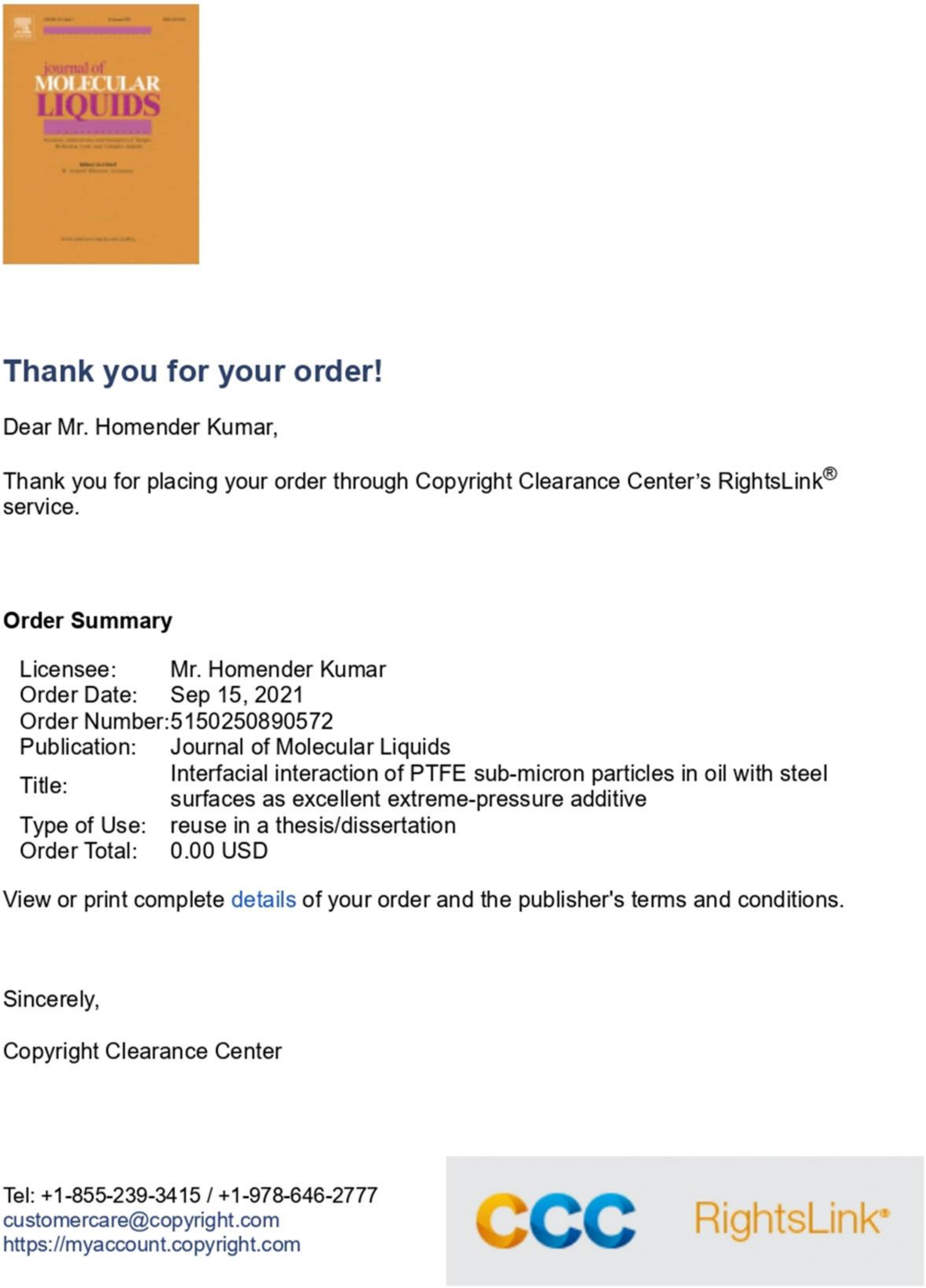

Thank you for your order!

Dear Mr. Homender Kumar,

Thank you for placing your order through Copyright Clearance Center's RightsLink® service.

Order Summary

Licensee:	Mr. Homender Kumar
Order Date:	Sep 15, 2021
Order Number:	5150250890572
Publication:	Journal of Molecular Liquids
Title:	Interfacial interaction of PTFE sub-micron particles in oil with steel surfaces as excellent extreme-pressure additive
Type of Use:	reuse in a thesis/dissertation
Order Total:	0.00 USD

View or print complete details of your order and the publisher's terms and conditions.

Sincerely,

Copyright Clearance Center

Tel: +1-855-239-3415 / +1-978-646-2777
customercare@copyright.com
https://myaccount.copyright.com

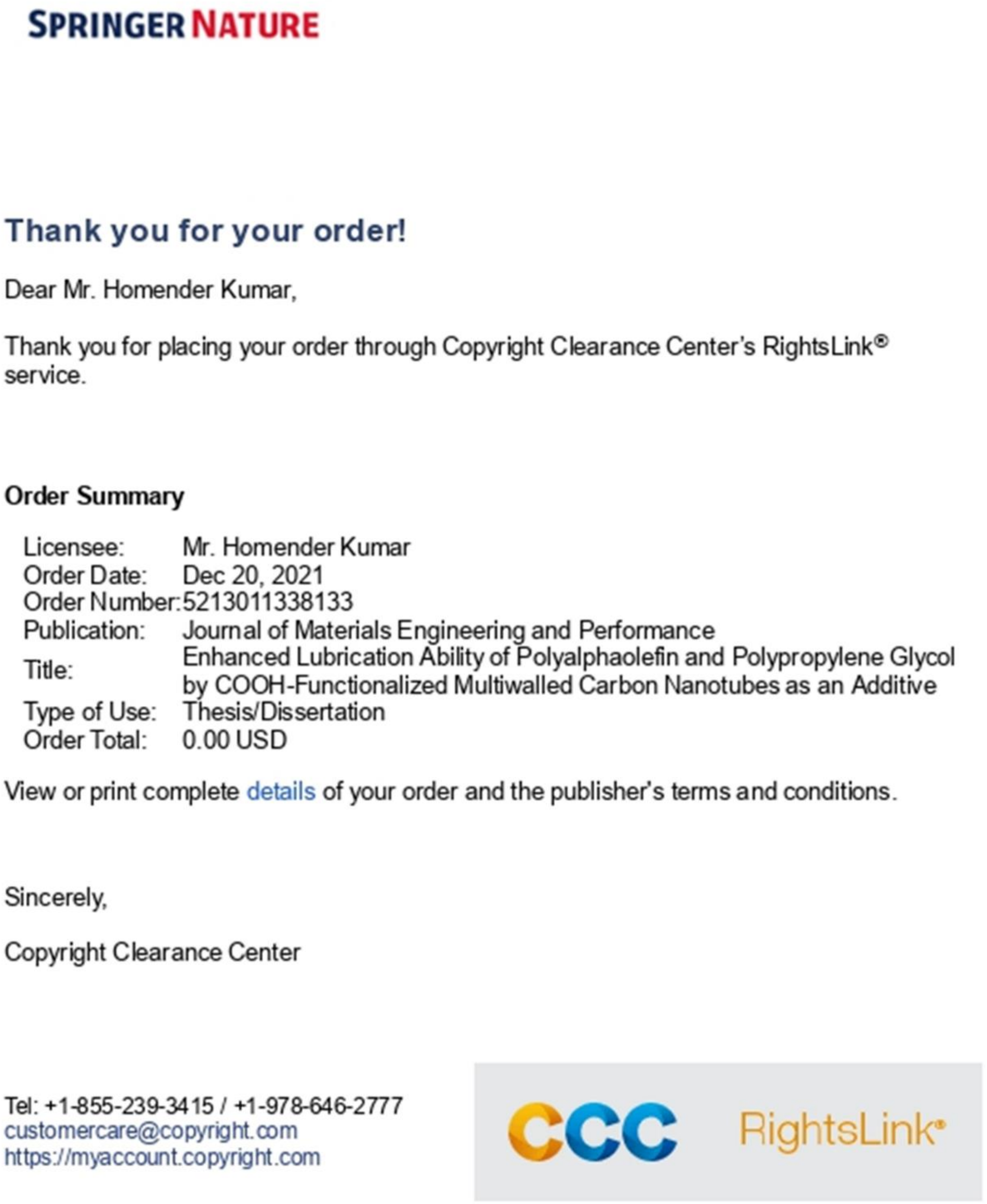

SPRINGER NATURE

Thank you for your order!

Dear Mr. Homender Kumar,

Thank you for placing your order through Copyright Clearance Center's RightsLink® service.

Order Summary

Licensee: Mr. Homender Kumar
Order Date: Dec 20, 2021
Order Number: 5213011338133
Publication: Journal of Materials Engineering and Performance
Title: Enhanced Lubrication Ability of Polyalphaolefin and Polypropylene Glycol by COOH-Functionalized Multiwalled Carbon Nanotubes as an Additive
Type of Use: Thesis/Dissertation
Order Total: 0.00 USD

View or print complete details of your order and the publisher's terms and conditions.

Sincerely,

Copyright Clearance Center

Tel: +1-855-239-3415 / +1-978-646-2777
customercare@copyright.com
https://myaccount.copyright.com

CCC RightsLink®

List of publications

a) Journal Publication

1. Kumar, H. and Harsha, A. P. (2020), "Investigation on Friction, Anti-Wear, and Extreme Pressure Properties of Different Grades of Polyalphaolefins with Functionalized Multi-Walled Carbon Nanotubes as an Additive," *Journal of Tribology,* 142(8), pp 081702–14. doi:10.1115/1.4046571
2. Kumar, H. and Harsha, A. P. (2021), "Enhanced Lubrication Ability of Polyalphaolefin and Polypropylene Glycol by COOH- Functionalized Multiwalled Carbon Nanotubes as an Additive," *Journal of Materials Engineering and Performance,* 30(2), pp 1075–1089. doi:10.1007/s11665-020-05450-0
3. Kumar, H. and Harsha, A. P. (2021), "Taguchi Optimization of Various Parameters for Tribological Performance of Polyalphaolefins Based Nanolubricants," *Proceedings of the Institution of Mechanical Engineers - Part J: Journal of Engineering Tribology,* 235(6), pp 1262–1280. doi:10.1177/ 1350650120972294
4. Kumar, H. and Harsha, A. P. (2021), "Augmentation in Tribological Performance of Polyalphaolefins by COOH- Functionalized Multiwalled Carbon Nanotubes as an Additive in Boundary Lubrication Conditions," *Journal of Tribology,* 143(10), pp 102202–14. doi:10.1115/1.4051392
5. Kumar, H., and Harsha, A. P., (2022), "Influence of Oleic Acid–Treated LaF 3 Nanoparticles as an Additive on Extreme Pressure Properties of Various Grades of Polyalphaolefins," *Tribology Transactions,* **65**(1), pp 96–113. doi: 10.1080/10402004.2021.2003495

b) Book Chapter

1. Kumar, H., and Harsha, A. P., (2021), "Group IV base stock -Polyalphaolefin a high-performance base oil for tribological applications," *Tribology and Sustainability*, CRC press, Taylor & Francis Group, pp: 163-188.

c) Publication in Conferences/Symposiums

1. Kumar, H., and Harsha, A. P., (2018), "Tribological behaviour of synthetic lubricants with functionalized Multiwalled Carbon nanotubes (MWCNT) as an additive," *TriboIndia-2018*, Veermata Jijabai Technical Institute, Mumbai, Maharashtra, India.
2. Kumar, H., and Harsha, A. P., (2019), "The role of COOH functionalized multiwalled carbon nanotubes as lubricant additive in different grades of polyalphaolefin oils," *IndiaTrib-2019*, Indian Institute of Science, Bangalore, Karnataka, India.
3. Kumar, H., and Harsha, A. P., (2020), "Wear inhibition performance of polyalphaolefins with oleic acid modified LaF_3 nanoparticles as an additive under extreme pressure conditions," *International Tribology Research Symposium (ITRS-2020)*, SRM Institute of Science and Technology, Kattankulathur, Tamil Nadu, Shri Mata Vaishno Devi University, J&K, and Centre for Advanced Studies, AKTU, Lucknow, India.
4. Kumar, H., and Harsha, A. P., (2020), "Anti-wear behaviour of polyalphaolefins with oleic acid-treated LaF_3 nanoparticles as an additive under extreme pressure conditions," *TriboIndia-2020*, SRM Institute of Science and Technology, Kattankulathur, Tamil Nadu, India.

Response sheet for the examiner's comment

Examiner-1

(a)	Table 1.1 correct the position of R in the structure of alkyl benzene	As per the examiner's suggestion, the position of R in the structure of alkyl benzene has been corrected.	The correct structure of alkyl benzene has been included in Table 1.1 (page no. 10)
(b)	Section 1.4 Role of additives in synthetic lubrication. The section title is broad-based, but the text is specific only to nano-additives. Please list the other additives used and their purpose. It gives the wrong impression that the final lubricant doesn't need additional additives other than nano-additives.	As per the examiner's suggestion, section 1.4 has been modified in the revised thesis.	Modifications are included in page no.12.
(c)	Please do a plagiarism check. (For example, load balancing page 7 matched almost exactly with the text at http://www.soil7.com/mobile/eng/knowledge/basic/function.jsp)	As per the examiner's suggestion, the plagiarism check has been done, and the thesis is modified wherever it is required.	Changes are included in page no. 7.
(d)	P64, section 2.9.3: The broad answers to the questions asked as a part of the Problem definition could be given in the summary. That will help in highlighting the main contributions of this work.	As per the examiner's suggestion, the overall conclusions regarding the problem definition have been included in the revised thesis.	The modifications have been included in section 8.2 on page 266.

Examiner-2

Comment No.	Questions	Reply to the comments	Remarks
1	The tabular summary of the literature survey is appreciated. This will serve as a good reference for future researchers. If it has not been published as a review paper, then these tables could be displayed on a website.	It has not been published as a review paper. However, the soft copy of the thesis will be available on the institute website under the e-resource of the library.	No changes are made in the revised thesis.
2	Rheological investigations of base oil+ nanoparticles were not carried out as it was assumed that the nanoparticles would have the least influence on viscosity. While that assumption may not be valid, certainly, the stability of the suspension to the shear rate would be an important contribution.	The authors reported rheological test only on neat PAOs because initial trial experiments with the LaF_3 as an additive did not significantly impact the rheological characteristics of PAOs and this may be because of the minimal concentration of additive (i.e., 0.025-0.15 wt.%) used in the test. Therefore, the authors provided the rheological characterization of only pure PAOs.	No changes are made in the revised thesis.
3	What are the reasons for using three different tribometers? What are the practical situations that are being simulated in these instruments? Maybe these questions can be addressed in chapter 3.	Bearing and engine components are encountered with various loads, speeds and motion at the contacting surface of the rubbing pairs. Therefore, three different tribometer were used to analyze the characteristics of lubricants under various sliding movements as well as under different lubrication conditions (i.e., fully flooded and starved)	The practical application of all tribometers has been included in respective section of chapter 3 i.e., section 3.5.1 (page no.77), section 3.5.2 (page no. 80) and section 3.5.3 (page no. 83)

4	The contact in most of the tribo-test is assumed to be elastic. This would mean that the contact pressure should not exceed Meyer's hardness (approx. three times yield stress) of the softest material in the contact pair. Please check this for all the tribo-contacts used. Reported contact pressures seem to be higher than the hardness.	The contact stress is calculated according to the Hertz theory considering elastic deformation characteristics. The classical theory of contact focused primarily on non-adhesive contact. The contact area is small compared to the sizes of the objects, and the stresses are highly concentrated in this area. The hertz contact pressure is different from nominal contact pressure. The anti-wear tests were conducted according to ASTM standards, and the calculated contact pressure (as reported in the thesis) is significantly higher than the hardness of steel. However, the lubricants were applied between the tribo-surfaces and thus formed a few nanometers thickness, separating the tribo-pairs and bearing the contact pressure. The pressures encountered in these contacts can be so high, and the rate of pressure rise so rapid that the lubricants are assumed to be squeezed out. The wear scar obtained in any typical test condition is very small. If the applied stresses are calculated for the given load, this will be less than the hardness of the steel.	The test has been conducted as per ASTM standards. Therefore, no change is required in the thesis. Further this will be clarified during viva-voce examination.
5	In general, it needs to be made clear that the results presented from chapter 4 onwards correspond to which tribometer. Section 4.1 title provides that detail but is missing elsewhere.	As per the examiner’s suggestion, details about the tribometer have been provided in the title of the respective section of the revised thesis (i.e., section 4.1 onwards).	The corrections have been included in page no. 161, 195 and 229.
6	What does the scatter bar indicate? Max/min or std dev? How many tests were carried out?	The scatter bar indicates the standard deviation. Each experiment was repeated thrice, and the average value of	Figure 4.4 (page no. 102), Figure 4.11 (page no. 118), and

	These details need to be provided for all the experiments.	these results was reported. The scatter bar has been provided for all the experiments.	Figure 7.4 (page no. 237) are corrected, and a modified figure is included in the revised thesis.
7	Sliding directions need to be indicated in all the SEM micrographs.	As per the examiner’s suggestion, all SEM micrographs have been provided with sliding direction.	Figure 4.5 is corrected and a modified figure is included in the revised thesis (page no. 106)
8	While measuring the 2D roughness profile, care should be taken on how the mean reference line (or curve if the specimen is a ball) is subtracted from the measured profile. The central flat/curved surface profile should be excluded while fitting the mean line. This needs to be done manually as the software included assumes a nominally flat surface.	In the present thesis work, the 2D roughness profile of worn surfaces are used to measure the depth of the wear scar (i.e., height difference) only.	No changes are made in the revised thesis.
9	In SRV-5 tests, the oscillation amplitude should be much larger than the contact diameter to ensure sliding. Has this condition been satisfied for all the loads used? Please check	The amplitude and frequency for given test conditions depend on the capability of the test rig. In the present study, tests were carried out as per ASTM D6425. The test condition has been satisfied for all the loads in the SRV-5 tribo-testing device.	No changes are required in the section 3.5.2 of chapter 3 of revised thesis. The details of ASTM standards have been given in the thesis.

10	In the accelerated tribo-tests as carried out in this work, the load and the velocity are chosen such that it simulates the actual experimental condition. Hence, they can be chosen as the input parameter for Taguchi method? In general, what are the assumptions behind this method and how the current conditions satisfy those conditions should be elaborated.	Since load and velocity are among the most important parameters that affect the tribological properties of lubricants. Hence, the load and velocity are chosen to investigate the influences of variation in input parameters on output parameters (COF and wear). The Taguchi method is based on fractional factorial design. So, it was assumed that the input variables are correlated to the response factor (output parameter) through a linear model. The responses are mainly affected by input factors and lower-order interactions, while higher-order interactions are relatively unimportant. Furthermore, it was also assumed that ambient temperature and relative humidity would remain constant for all tests. As explained in the thesis, the confirmation test validates all assumptions and conditions taken into account while applying the Taguchi method.	No changes are made in the revised thesis.
11	Generally, tribology is about detecting anomalous behavior in otherwise a steady-state experiment. A crack propagation, removal of a chunk of material, breakage of the protective film, and other such events dictate the tribological behavior. I think Taguchi method assumes a steady deviation from the steady-state process. Please verify.	Taguchi method does not assume a steady deviation from the steady-state process. Taguchi method’s primary purpose is to reduce the variability around the target value while simultaneously guiding the performance towards optimal combination of input parameters. The confirmation test can verify the above statements as explained in the thesis.	No changes are made in the revised thesis.
12	What are the dotted lines in the bear area curves? Why are the parameters defined with	The dotted line is used to illustrate the various parameters as explained in the thesis. The dotted lines are only used to differentiate between the tangent drawn on the BAR curve	Figure 6.9 is corrected, and a modified figure is

	respect to the dotted lines instead of the actual curves?	and other parameters. Therefore, there is no physical significance of dotted lines.	included in the revised thesis (page no. 215)
13	What is the effect of the AFM tip radius on the peak and valleys of the topography? Any attempt made to estimate the tip radius?	The AFM tip radius was constant, i.e., 10 nm. Therefore, no attempt was performed to analyze the effect of AFM tip radius on the peak and valleys. This is the limitation of this thesis work.	No change is made in the revised thesis.
14	AFM scans a small area. When the worn area has inhomogeneous topography choosing the area for AFM scan becomes very important. No details on how this was done is given.	The AFM used in the present thesis work has scanned the arbitrary area (60×60 μm^2) of the worn surface of steel balls. Based on the worn scan area, the wear mechanism was explained.	No changes are made in the revised thesis.
15	Why is the rheological properties of the PAO spread over two different chapters?	The primary purpose of the rheological characterizations of PAOs is to support the tribological test results. Therefore, it was explained in two different chapters.	No changes are made in the revised thesis.
16	Overall, a lot of experimental work has been carried out. However, it is not clear what the main contributions that will help the lubricant designers are? Most of the results are specific to the tests that have been carried out, and no attempt has been made to generalize the results in terms of identifying the underlying mechanisms. If these shortcomings had been addressed, this thesis would have been much better.	The effect of different concentrations of two different nano-additives on tribological characteristics will undoubtedly help the lubricant designer. The results show the performance of lubricants under different tribological test conditions. The authors have attempted to explain the underlying mechanisms in various tribological test conditions wherever necessary in the present thesis work.	No changes are made in the revised thesis.